Journal of Alloys and Compounds 506 (2010) 811–814

Contents lists available at ScienceDirect

Journal of Alloys and Compounds

journal homepage: www.elsevier.com/locate/jallcom

Preparation and characterization of $Li_5ReSi_4O_{12}$ (Re = Nd, Gd) solid electrolyte

Chenghuan Huang, Kelong Huang*

School of Chemistry and Chemical Engineering, Central South University, Changsha 410083, China

ARTICLE INFO

Article history:
Received 7 May 2010
Received in revised form 7 July 2010
Accepted 8 July 2010
Available online 15 July 2010

Keywords:
Solid electrolyte
Solid-state reaction
Conductivity
Electrochemical impedance spectroscopy

ABSTRACT

Dense $Li_5ReSi_4O_{12}$ (Re = Nd, Gd) ceramic materials with densities of 3.0–3.1 g/cm^3 were synthesized by a solid-state reaction method. The samples were characterized by X-ray diffraction (XRD), scanning electron microscopy (SEM) and electrochemical impedance spectroscopy (EIS). The conductivity of $Li_5NdSi_4O_{12}$ was 1.2×10^{-2} mS/cm at 550 °C and 2.5×10^{-4} mS/cm at 350 °C, respectively, with activation energy of 0.84 eV. $Li_5GdSi_4O_{12}$ with activation energy of 0.90 eV had conductivities similar to $Li_5NdSi_4O_{12}$, suggesting that neither rare earth ion significantly affected the properties of $Li_5ReSi_4O_{12}$.

1. Introduction

Li-ion conducting solids are materials of increasing interest because of their possible use as solid electrolytes in high-energy solid-state batteries [1–4]. Liquid-free batteries have various advantages over currently commercialized ones. These include safety issues caused by flammable organic electrolytes and irreversible capacity loss during cycles and storage originated by the solid electrolyte interface [5–7]. Therefore, solid-state electrolytes with chemical stability and high ionic conductivity have been considered as candidates to substitute liquid organic electrolytes in Li-ion batteries.

A wide variety of inorganic materials, such as sulfides [4,8,9], hydride-based materials [10–12], and perovskite-type (ABO_3) oxides (A = Li, La and B = Ti) [1,13], have been found to exhibit high lithium ionic conductivity for low temperature application. On the other hand, recent studies on high temperature Li-ion conductors are also attracting attention in order to develop high temperature batteries [14–16] and other electrochemical devices [17]. Some lithium rare earth silicates ($LiLnSiO_4$, Ln = La–Dy) with apatite structure have thermal stability and relatively high conductivity at over 500 °C [18]. Furthermore, NASICON-type alkali rare earth silicates, such as $Na_5ReSi_4O_{12}$ (Re = rare earth metal) [19,20] and $Na_{3+3x-y}Re_{1-x}P_ySi_{3-y}O_9$ [21,22], show excellent ionic conductivity. For instance, the ionic conductivity of $Na_5ReSi_4O_{12}$ is over 10^{-2} S/cm at 300 °C [20]. Such a structure consists of $Si_{12}O_{36}$ metasilicate rings stacked along the threefold axes of the rhombohedral space group. Na^+ ions in the sites between the rings are mobile, resulting in the super ionic conductivity [19]. For this reason, we attempted to synthesize Li-substitution $Na_5ReSi_4O_{12}$-type of materials ($Li_5ReSi_4O_{12}$, Re = Nd, Gd), and characterized their properties.

2. Experimental

$Li_5NdSi_4O_{12}$ powder was synthesized by a solid-state reaction method. Stoichiometric amounts of high-purity Li_2CO_3, Nd_2O_3 and SiO_2 powders were mixed by ball milling in ethanol for 48 h, followed by drying in an oven and calcination at 850 °C for 12 h in air. The calcinated powder was ground and mixed again, followed by the second calcination under the same conditions as the first time. The sample was cooled to room temperature, ground and manually pelletized using a disk-shaped mold. The pellets were sintered at 960 °C for 6 h in air to get dense ceramic materials. The final products of $Li_5NdSi_4O_{12}$ were blue. The overall reaction for formation of $Li_5NdSi_4O_{12}$ is given by the following reaction:

$$5Li_2CO_3 + Nd_2O_3 + 8SiO_2 \xrightarrow{\Delta} 2Li_5NdSi_4O_{12} + 5CO_2 \qquad (1)$$

A similar synthesis method was applied to prepare $Li_5GdSi_4O_{12}$ powder and ceramic. However, the final products of $Li_5GdSi_4O_{12}$ were white.

The morphology of the samples was revealed by using scanning electronic microscopy (SEM, LEO 1530). The crystal structure and phase purity was analyzed by using X-ray diffraction pattern (XRD, X'Pert PRO Alpha-1). Conductivity measurements from 300 to 550 °C were carried out with AC electrochemical impedance spectroscopy (EIS) by using a Solarton 1255 impedance analyzer with a Solarton 1287 electrochemical interface in the frequency range of 10 Hz to 5 MHz, with an AC perturbation voltage of 10 mV. Conductive silver paint was used as electrodes. Ionic conductivity values were calculated with $\sigma = d/(R \times S)$, where d denotes the sample thickness, S the area of the electrodes and R the sample resistance, which can be obtained from complex impedance plots.

---

* Corresponding author. Tel.: +86 73188879850; fax: +86 73188879850.
E-mail address: huangkelong@yahoo.com.cn (K. Huang).

0925-8388/$ – see front matter © 2010 Elsevier B.V. All rights reserved.
doi:10.1016/j.jallcom.2010.07.078

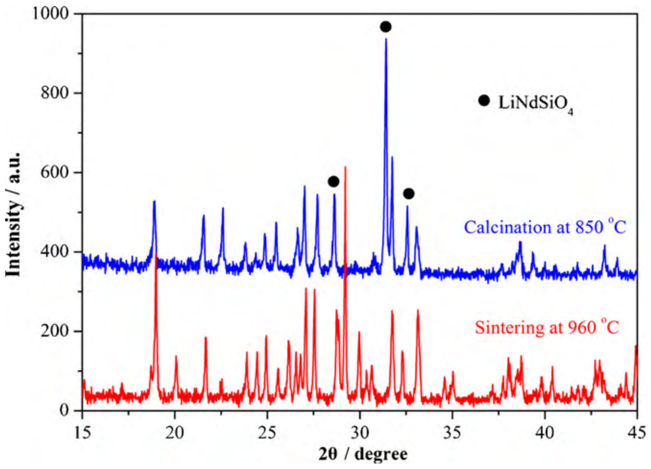

Fig. 1. XRD patterns of $Li_5NdSi_4O_{12}$ after calcination and sintering.

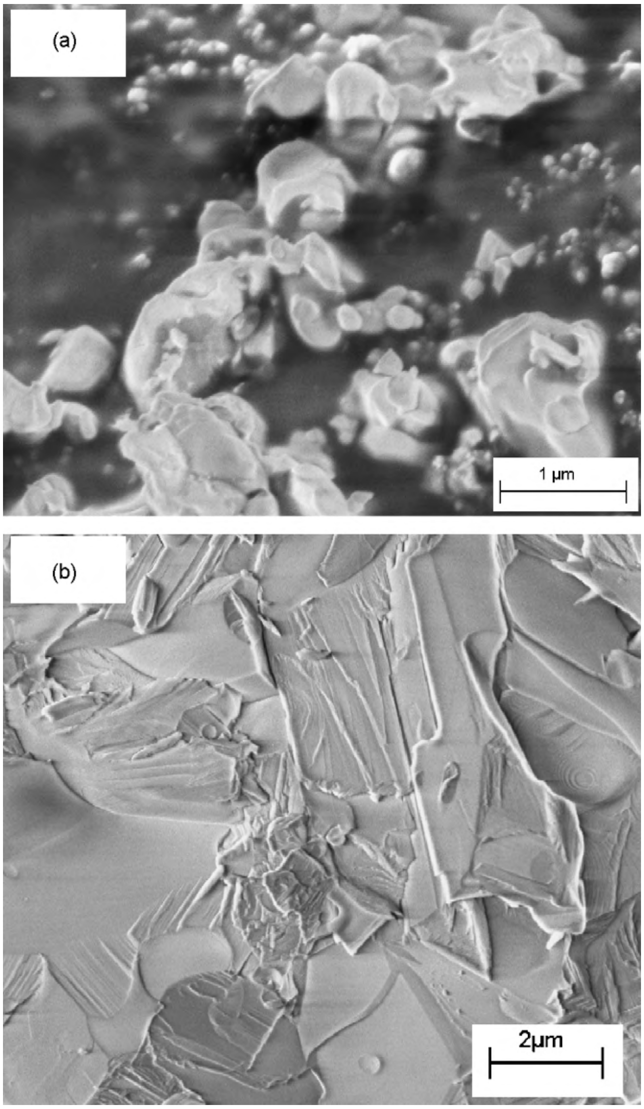

Fig. 2. SEM images of $Li_5NdSi_4O_{12}$ after (a) calcination at 850 °C and (b) sintering at 960 °C, respectively.

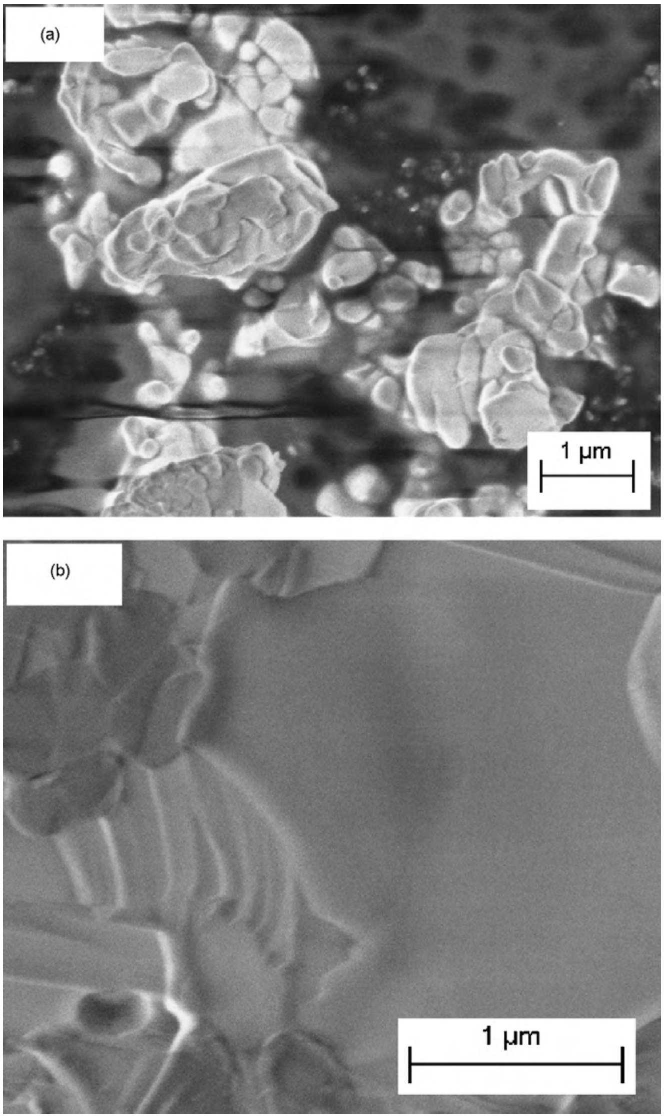

Fig. 3. SEM images of $Li_5GdSi_4O_{12}$ after (a) calcination at 880 °C and (b) sintering at 980 °C, respectively.

3. Results and discussion

Fig. 1 shows the XRD pattern of $Li_5NdSi_4O_{12}$ after calcination and sintering. No peak of Li_2O, Nd_2O_3, or SiO_2 was found. However, the peaks of $LiNdSiO_4$ were detected after the first calcination, indicating that the solid-state reaction was not completed. Repeating grinding and mixing of the sample would facilitate the solid reaction. After the sample sintered at 960 °C, the peaks of $LiNdSiO_4$ disappeared. Fig. 2 shows SEM images of the $Li_5NdSi_4O_{12}$ powder and pellet, respectively. The grain sizes of $Li_5NdSi_4O_{12}$ after calcination at 850 °C were 200 nm to 1 μm. The cross-section image shows that the pellet was dense after sintering. The density of the ceramic was 3.0 g/cm^3. Fig. 3 shows that the grain size distribution of $Li_5GdSi_4O_{12}$ powder was also in the range of 200 nm to 1 μm. Likewise, the $Li_5GdSi_4O_{12}$ pellet was dense after sintering, with a density of 3.1 g/cm^3.

Fig. 4 shows typical AC impedance spectra of both $Li_5NdSi_4O_{12}$ and $Li_5GdSi_4O_{12}$ pellets at different temperatures. In Fig. 4(a), the impedance of $Li_5NdSi_4O_{12}$ is associated with the large semicircle starting from the origin and ending at about $1.6 \times 10^4\ \Omega$, implying that the resistance of the $Li_5NdSi_4O_{12}$ specimen was about $1.6 \times 10^4\ \Omega$ at 550 °C. The impedance of the specimen increased

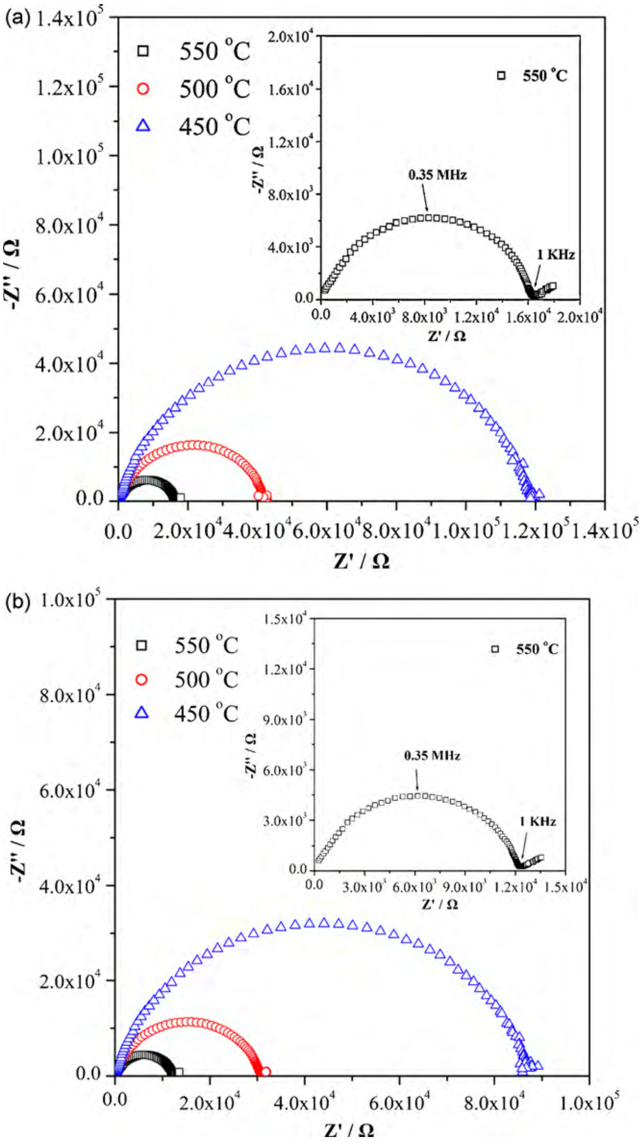

Fig. 4. Impedance spectra of (a) $Li_5NdSi_4O_{12}$ and (b) $Li_5GdSi_4O_{12}$ pellets at different temperatures.

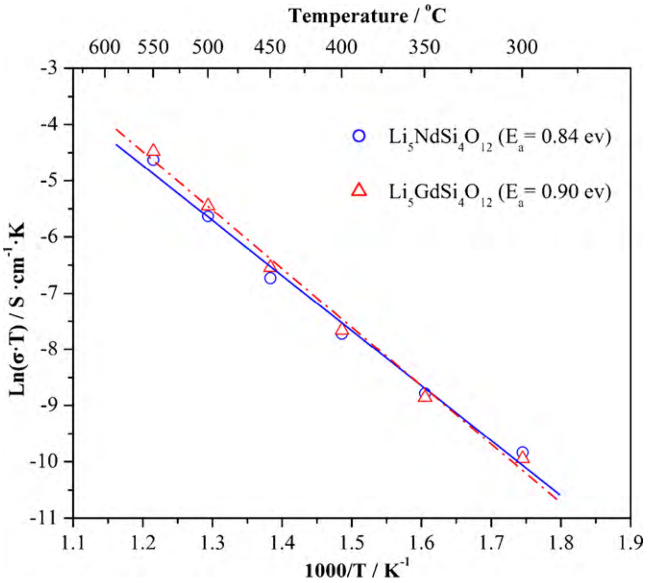

Fig. 5. Arrhenius plots of conductivity as a function of absolute temperature for $Li_5NdSi_4O_{12}$ and $Li_5GdSi_4O_{12}$.

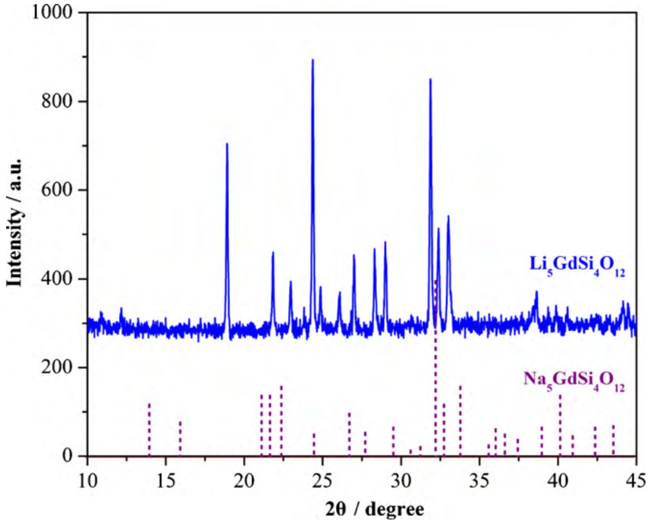

Fig. 6. XRD pattern of $Li_4GdSi_4O_{12}$ after sintering at 980 °C.

with decreasing measured temperatures. The conductivity was 1.2×10^{-2} mS/cm at 550 °C and 2.5×10^{-4} mS/cm at 350 °C, respectively. $Li_5GdSi_4O_{12}$ had similar impedance spectra with those of $Li_5NdSi_4O_{12}$, as shown in Fig. 4(b), with a conductivity of 1.4×10^{-2} mS/cm at 550 °C and 2.3×10^{-4} mS/cm at 350 °C, respectively. The close conductivity of the two samples infers that the rare earth elements with different radii are not a significant influence on the conductivity of $Li_5ReSi_4O_{12}$, although the conductivity of NASICON depends on the size of rare earth ions [20].

The conductivity, σ, obeys the Arrhenius equation:

$$\sigma \cdot T = A \exp\left(\frac{-E_a}{K_B T}\right) \quad (2)$$

where T is the absolute temperature, A the pre-exponential factor, E_a the activation energy for conduction, and k_B the gas constant. The conductivity obtained at each temperature was plotted as $\ln(\sigma \cdot T)$ *vs.* $1000/T$ in Fig. 5, which indicates a linear feature for both samples. According to the Arrhenius relation, the activation energy E_a of $Li_5NdSi_4O_{12}$ and $Li_5GdSi_4O_{12}$ was 0.84 and 0.90 eV, respectively, which is higher than that of corresponding $Na_5ReSi_4O_{12}$-type NASICON. The E_a of $Na_5GdSi_4O_{12}$ was in the range of 0.24–0.31 eV, as reported in Ref. [20]. Li^+ has a smaller radius than Na^+, which may lead to the change of the $Na_5GdSi_4O_{12}$-type structure after the substitution of Li^+ for Na^+, as shown in Fig. 6, resulting in lower ion mobility in $Li_5GdSi_4O_{12}$ than in $Na_5GdSi_4O_{12}$. However, the conductivity of $Li_5GdSi_4O_{12}$ at 550 °C is about 10^3 times greater than that of $LiSmSiO_4$ [14].

4. Conclusions

$Li_5ReSi_4O_{12}$ (Re = Nd, Gd) powders with grain sizes of 200 nm to 1 µm were prepared by a simple solid-state method. For $Li_5NdSi_4O_{12}$, XRD and SEM results showed that impurity of $LiNdSiO_4$ disappeared and $Li_5NdSi_4O_{12}$ ceramic became dense after sintering at 960 °C. The dense ceramic with a density of 3.0 g/cm^3 had an ionic conductivity of 1.2×10^{-2} mS/cm at 550 °C. Similarly, $Li_5GdSi_4O_{12}$ with a density of 3.1 g/cm^3 had an ionic conductivity of 1.4×10^{-2} mS/cm at 550 °C. The activation energy of $Li_5NdSi_4O_{12}$ and $Li_5GdSi_4O_{12}$ was 0.84 and 0.90 eV, respectively. Neither rare earth ion had a significant impact on the properties of $Li_5ReSi_4O_{12}$.

Acknowledgement

The authors would like to thank Dr. M.L. Liu for his suggestions.

References

[1] J.W. Fergus, J. Power Sources 195 (2010) 4554.
[2] M. Kotobuki, Y. Suzuki, H. Munakata, K. Kanamura, Y. Sato, K. Yamamoto, T. Yoshida, J. Electrochem. Soc. 157 (2010) A493.
[3] A. Mei, Q.-H. Jiang, Y.-H. Lin, C.-W. Nan, J. Alloys Compd. 486 (2009) 871.
[4] J.E. Trevey, Y.S. Jung, S.-H. Lee, J. Power Sources 195 (2010) 4984.
[5] L.C. Yang, W.L. Guo, Y. Shi, Y.P. Wu, J. Alloys Compd. 501 (2010) 218.
[6] S. Menkin, D. Golodnitsky, E. Peled, Electrochem. Commun. 11 (2009) 1789.
[7] C.C. Huang, K.L. Huang, S.Q. Liu, Y.Q. Zeng, L.Q. Chen, Electrochim. Acta 54 (2009) 4783.
[8] H. Yamane, M. Shibata, Y. Shimane, T. Junke, Y. Seino, S. Adams, K. Minami, A. Hayashi, M. Tatsumisago, Solid State Ionic 178 (2007) 1163.
[9] Y. Nishio, H. Kitaura, A. Hayashi, M. Tatsumisago, J. Power Sources 189 (2009) 629.
[10] H. Maekawa, M. Matsuo, H. Takamura, M. Ando, Y. Noda, T. Karahashi, S. Orimo, J. Am. Chem. Soc. 131 (2009) 894.
[11] M. Matsuo, A. Remhof, P. Martelli, R. Caputo, M. Ernst, Y. Miura, T. Sato, H. Oguchi, H. Maekawa, H. Takamura, A. Borgschulte, A. Züttel, S. Orimo, J. Am. Chem. Soc. 131 (2009) 16389.
[12] M. Matsuo, H. Takamura, H. Maekawa, H.-W. Li, S. Orimo, Appl. Phys. Lett. 94 (2009) 084103.
[13] J. Wolfenstine, J.L. Allen, J. Read, J. Sakamoto, G. Gonalez-Doncel, J. Power Sources 195 (2010) 4124.
[14] M. Ganesan, M.V.T. Dhananjeyan, K.B. Sarangapani, N.G. Renganathan, J. Alloys Compd. 450 (2008) 452.
[15] M. Ganesan, Electrochem. Commun. 9 (2007) 1980.
[16] M. Ganesan, J. Appl. Electrochem. 39 (2009) 5.
[17] S. Nakayama, K. Onishi, T. Asahi, Y.L. Aung, S. Kuwata, Ceram. Int. 35 (2009) 3057.
[18] M. Sato, Y. Kono, H. Ueda, K. Uematsu, K. Toda, Solid State Ionic 83 (1996) 249.
[19] H.U. Beyeler, T. Hibma, Solid State Commun. 27 (1978) 641.
[20] R.D. Shannon, B.E. Taylor, T.E. Gier, H.Y. Chen, T. Berzins, Inorg. Chem. 17 (1978) 958.
[21] K. Yamashita, M. Tanaka, T. Kakuta, M. Matsuda, T. Umegaki, J. Alloys Compd. 193 (1993) 283.
[22] T. Okura, H. Monma, K. Yamashita, J. Eur. Ceram. Soc. 26 (2006) 619.